JOURNAL OF MATERIALS SCIENCE **38** (2003) 2019–2025

Bulk and interior packing densities of random close packing of hard spheres

YUGONG WU, ZHIGANG FAN, YUZHU LU
School of Electronic and Information Engineering, Tianjin University, Tianjin 300072, People's Republic of China
E-mail: wuyugong@eyou.com

The packing densities of random close packing of equal hard spheres (RCPHS) are studied. The RCPHS is generated by a rearrangement algorithm with an optimization subroutine. Traditionally defined packing density, bulk density, is found to be 0.635 ± 0.002 by extrapolation to infinite number of spheres. We propose that there exist a characteristic packing density without boundary effects. This interior packing density is calculated by two methods, resulting in values without statically significant difference. Interior packing density deduced from Voronoi diagram is 0.6690 ± 0.0006. Local packing density for each sphere is defined as ratio of its volume to volume of its corresponding Voronoi cell and is sensitive to sphere's local configuration and overlapping.

1. Introduction

Random close packing of hard spheres (RCPHS) is a useful model for various physical systems such as liquids, glasses, powders and colloidal suspensions [1–3]. There are extensive studies on RCPHS, which can be classified into two catalogues. Numerous experiments were carried out, in which physical spheres of steel or nylon, etc., were poured into containers of different shapes and volumes [4–7]. Packing densities, which are the ratios of the total volume of spheres to the volume of containers, are measured and coordination number of spheres was also recorded in some experiments. When equal spheres were poured into rigid containers, there appeared to be a range of random packing density possible, with the upper limit at 0.637 and the lower limit at 0.601 [5]. Reported packing density of RCPHS of equal radius with the highest precision was 0.6366 ± 0.0005 [7]. There are questions accompanying with the interpretation of results of such experiments [7]. It was observed that there was tendency of the formation of some almost regular packing at the walls of the container, especially when they were even planes. Additional void space also appeared at the walls. The two kinds of boundary effects just mentioned influence the value of packing density in opposite directions, and, therefore, a rather crude experiment could yield out result that was fairly close to those from more elaborate measurements. It seems that traditionally defined packing density alone, even if it was obtained through extrapolation of measured data to infinite container volume, cannot reveal the packing density of RCPHS without ambiguity. The other catalogue of RCPHS studies relies on computer simulation. Packing of spheres with definite radius distribution is generated by computer algorithms [8–12]. Because location and radius of spheres are recorded completely, it is relatively easy to perform detailed structure analysis. Radial distribution functions (RDFs) and Voronoi polyhedra analysis were frequently reported to reveal the connectivity of spheres [11, 12]. The same difficulty in utilization of packing density as an indicator of the packing nature also exists due to the boundary effects. In fact, packing density as high as 0.665 was reported for RCPHS of equal spheres [13].

Computer algorithms used to generate RCPHS can be further classified into two catalogues [14]. The first is the sequential generation method [8, 9]. By this method, only one particle is generated each time and added to the surface of cluster of spheres existing already based on some criteria. The second is the collective rearrangement algorithms [10–14], where many spheres are initially placed randomly within a defined space, with overlaps between neighboring spheres. An algorithm was then applied to relocate each sphere to new position to reduce the overlaps between spheres. When such an algorithm could not further decrease the overlapping volume, all spheres were shrunk by a factor. By repeating the relocation and shrinking steps, an overlapping free packing was finally obtained. The most important feature of relocation algorithm was how new position of the sphere in consideration was decided. Usually, if a sphere had overlaps with n surrounding spheres, its new position after the specific relocation operation is determined by a linear combination of its initial coordinates and that of n neighbors. Since the overlap volume had a dimension of three (length^3) while that of coordinate a dimension of one (length), some proposed relocation operations would in fact increase the overlap volume and therefore could not be performed, while it was rare for other operations to result in minimum overlapping

volume possible, even though they do decrease it. Enormous iterations were needed to get overlapping free packing. It was found that some spheres might be locked into place and decrease of radii would not change the local structure. To prevent occurrence of this situation, each sphere should take a small random displacement, imitating vibration process in packing experiments. It was highly experiential to decide when and how to vibrate spheres. Long range ordering of spheres could also appear in vicinity to boundary without appropriate random displacement [15].

In this paper, we modified the traditional rearrangement algorithm by a straightforward approach to the reduce of overlapping volume. An optimization subroutine is employed to find the minimum overlapping position for each sphere to be relocated. Vibration process is eliminated. Ordering near boundary is avoided through allocation of boundary condition for each sphere in optimization subroutine. Packing of spheres of equal radii obtained will be analyzed and compared with results in literature. We concentrate our discussion on the definition and calculation of various kinds of packing densities and the concepts of bulk and interior packing densities is proposed which provide insight of nature of RCPHS.

We first give a description of our algorithm of RCPHS simulation, and then a detailed presentation of the analysis of RCPHS of equal radius. A summary is listed at the end of this paper.

2. Algorithm to generate RCPHS

Given below is an outline of the computer algorithm used in this work to generate RCPHS (Fig. 1), some key parameters involved are also presented.

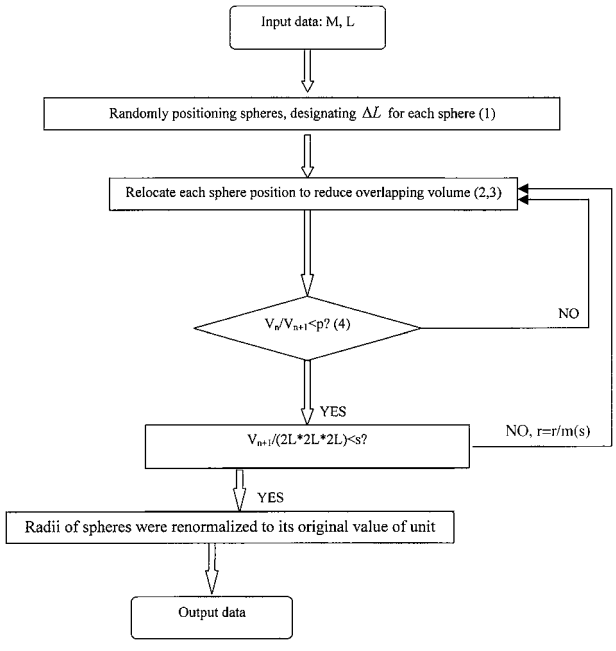

Figure 1 Algorithm to generate RCPHS. Variables are defined in text. Numbers in parentheses correspond to steps described in Section 2 with same notation.

(1) M points of uniform distribution are placed in a cubic domain of size $2L*2L*2L$. These points sever as initial center of M spheres. Simulation results show that stable statistical properties can be obtained with $M \geq 5,000$ [16]. In this paper we present results from RCPHS of 10,000 spheres. Initially, radius of each sphere is unity, leading to an overlapping volume, V, of the order of 10^4.

At the beginning of this work, we found that ordered cluster seeded easily at the domain boundary during relocation process and grew into interior. To avoid the occurrence of long range ordering, we assigned another constraint to space available for spheres. Each sphere should move within a quasi-cube of size $2L+\Delta L$, where ΔL are different for different spheres and uniformly distributed in the range from $-r/2$ to $+r/2$. Of course, this constraint is effective only to spheres near initial cubic domain of size $2L*2L*2L$. In other word, the initial even planar boundary is transformed into rough boundary through utilization of this constraint and ordering near the boundary is avoided.

(2) The spheres were relocated one by one in a random sequence to reduce V. When a specific sphere of radius r is in consideration, no other spheres are allowed to move. An optimization subroutine finds a new position for this sphere within the spheric space with a radius of $2r$ centered at its original center and, at the same time, within the quasi-cube, to minimize its overlapping volume with surrounding spheres. After each sphere is relocated, V reaches a new lower value.

(3) Overlapping volume of a sphere with its neighbor is a non-linear function of its coordinates. In construction of RCPHS, this overlapping volume is to be minimized under constraint conditions. An efficient algorithm for this kind of problem is to solve corresponding Kuhn-Tucker equation through sequential quadratic method [17] and is employed in our program.

(4) This relocation step is iterated (each iteration having different random sequence of spheres), until no signification reduction of V can be achieved. The ratio of overlapping volumes of two successive iteration, $p = V_n/V_{n+1}$, is assumed to be the criterion to determine whether the overlapping volume is reduced significantly and the critical value of p (p_c) is 1.0005 in this work. When p is less than the critical value, the relocation step is executed again.

(5) All radii of spheres are shrunk by a factor of m, if relocation of spheres cannot reduce overlapping volume significantly. In this case, times of shrunk of spheres, N_p, is counted. In this work, m is 1.0003.

(6) Relocation process is terminated when overlapping volume satisfies a standard s, overlapping ratios, which is defined as (overlapping volume/$(2L)^3$). Radii of spheres were renormalized to its original value of unity and their centers linearly transformed using N_p and m.

We also performed a series of simulations to record configurations of 10,000 spheres to find out which s value reproduces RCPHS characteristics reported in literatures. Finally, a RCPHS of M spheres is obtained. For M = 10,000, all spheres positioned in

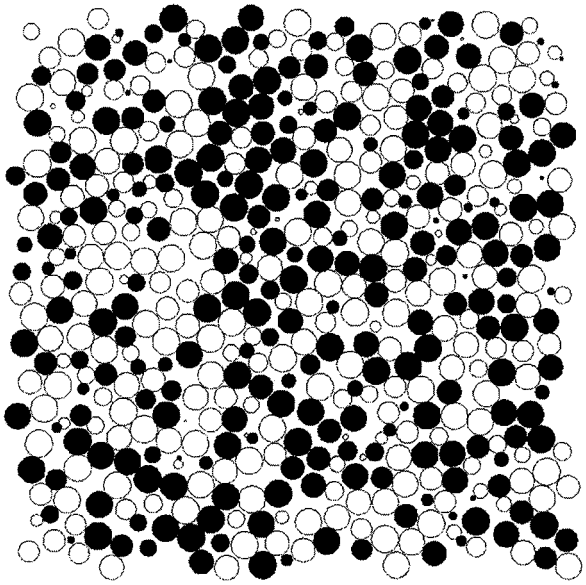

Figure 2 A typical cross section of RCPHS. The centers of the shaded spheres are above the cross section plane while the others are under the cross section plane.

an approximately cubic domain of size about $(2L)^3 = 40 * 40 * 40$ (the original value of 2L is 30) and overlapping volume is less than $s * (2L)^3$. A typical cross section of RCPHS is showed in Fig. 2.

Simulation of RCPHS is carried out in a personal computer with CPU of 1 GHz. It takes approximately 80 hrs CPU time to generate a RCPHS of 10,000 spheres.

3. Results and discussion

Five sets of RCPHS with 10,000 spheres each are simulated. To eliminate possible boundary effects near domain boundary due to our algorithm, spheres centered within outermost shell of two times sphere diameters (four length unit) thick are not included in analysis below.

3.1. Radial distribution function

Radial distribution functions (RDF) corresponding to overlapping ratios s from $1 * 10^{-5}$ to $2 * 10^{-3}$ is calculated (Fig. 3). At the overlapping ratio from $7.5 * 10^{-5}$ to $6.0 * 10^{-4}$, the RDFs exhibit a first peak at one diameter and a split second peak with the first subpeak lower than the second one. The first subpeak locates at 1.744 diameter (expected value is $\sqrt{3}$), while the second one at 1.993 diameter for $s = 7.5 * 10^{-5}$. The first subpeak locates at 1.721 diameter while the second one at 1.970 diameter for $s = 6.0 * 10^{-4}$. A lower subpeak position indicates overlapping of spheres and a higher position departure of spheres. However, when the overlapping ratio is greater than $5 * 10^{-4}$, the first subpeak of the split second peak is higher than the second one, contradictious to RCPHS feature reported in literature [11, 12] and the first subpeaks move gradually to lower position (e.g., at 1.653 diameter when $s = 6.4 * 10^{-3}$). At s value equal to or less than $1.0 * 10^{-4}$, the first subpeak locates higher than 1.74. Judged by RDF, RCPHS

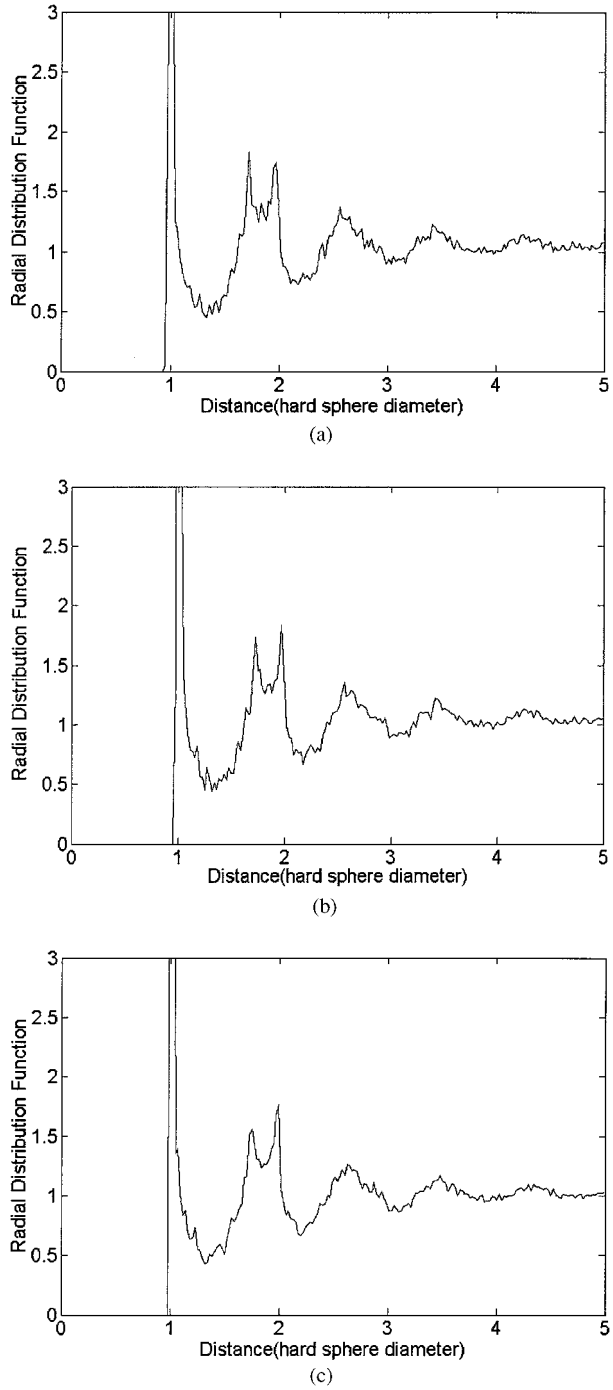

Figure 3 Radial distribution function of RCPHS with different overlapping ratio (a) $s = 6.0 * 10^{-4}$, (b) $s = 5.0 * 10^{-4}$, and (c) $s = 1.0 * 10^{-4}$.

feature can be obtained with s ranging from $2.0 * 10^{-4}$ to $5 * 10^{-4}$ and our simulation leads to a local structure of random close packing similar to those generated by algorithms without optimization subroutine.

3.2. Bulk packing density

Suppose that a virtual hard spherical container is placed in the RCPHS structure and only those spheres that totally within the container will contribute to the calculation of the sum of the volume of spheres (Fig. 4a). This is the situation encountered in packing experiments. When the radius of the container is changed gradually, packing density ρ_1, defined as ratios of volume

of the spheres within the container to the volumes of container, evolves into an asymptotic value (Fig. 5a) According to theory [4], there exists the relationship between ρ_1, and N, the number of spheres as

$$\rho_1(N) = \rho_{1\infty} + AN^{-\frac{1}{3}} \tag{1}$$

where $\rho_{1\infty}$ is the extrapolation value of $\rho_1(N)$ as $N \to \infty$ (infinite number of spheres). The relation between $\rho_{1\infty}$ and overlapping ratio s is shown in Fig. 5b in semi-log plot. When s is greater than 10^{-3}, $\rho_{1\infty}$ decreases steeply with the decrease of s. This is obviously due to the reduce of overlapping between spheres. When s is less than $1 * 10^{-4}$, $\rho_{1\infty}$ reaches value much lower than 0.63. At this stage shrinkage of radii results that many spheres are not in contact with its neighbors. Above explanation is consistent with observed evolution of the position of subpeaks in RDF. Present work shows clearly the limitation of relocation method to simulate RCPHS structure. It is difficult to get s less than 10^{-4} without loosing the structure.

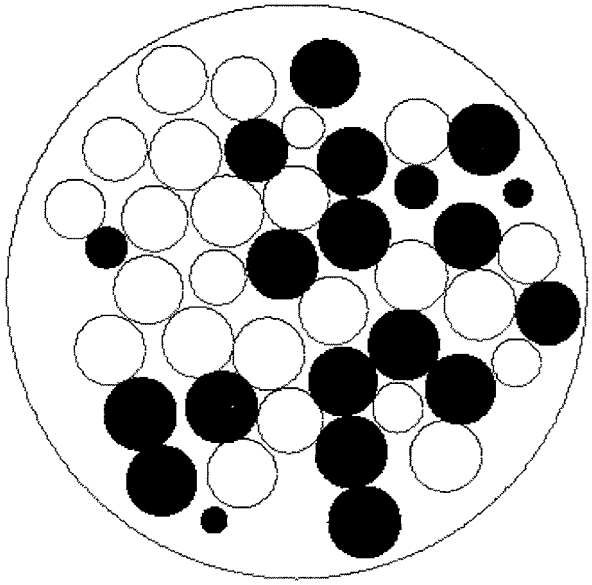

(a)

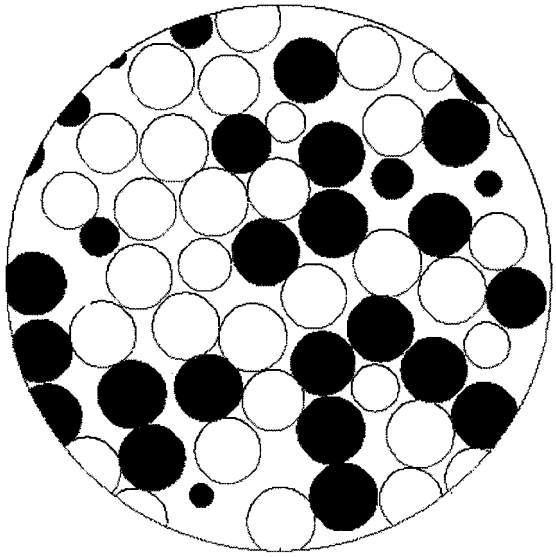

(b)

Figure 4 Cross sectional schematic illustration of definition of (a) packing density ρ_1, (b) packing density ρ_2, and (c) packing density ρ_z where each polygon presents a Voronoi cell within which lays a sphere (but not necessarily sectioned by the plane). The centers of the shaded spheres are above the cross section plane while the others under the cross section plane. (*Continued*)

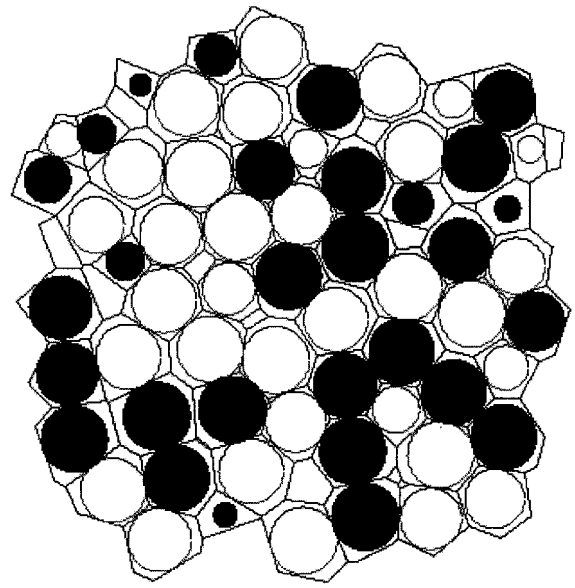

(c)

Figure 4 (*Continued*).

Evolution of $\rho_{1\infty}$ with s from $1 * 10^{-4}$ to $9 * 10^{-4}$ is shown in Fig. 5c in linear plot. When $s = 3 * 10^{-4}$, $4 * 10^{-4}$ or $5 * 10^{-4}$, we have $\rho_{1\infty}$ values between 0.63 and 0.64. $\rho_{1\infty}$ begins to drop abruptly with s less than $4 * 10^{-4}$. This feature, besides the consideration of RDF, lead us to prefer s equal to $4 * 10^{-4}$ or $5 * 10^{-4}$ as the suitable standard to be adopted in our algorithm. All the data below are obtained at s equal to $5.0 * 10^{-4}$.

By standard curve fitting technique, we have an average value of $\rho_{1\infty} = 0.6352$ with a standard deviation of 0.0016 and an average value of $A = -1.120$ with a standard deviation of 0.016. It should be noted that one kind of boundary effect on packing density, i.e., possible ordering of spheres on container's wall, is avoided in calculation of $\rho_{1\infty}$ by using virtual container. The other kind of boundary effect that additional void exits on boundary still retains. So, $\rho_1(N)$ and $\rho_{1\infty}$ are bulk packing densities of RCPHS.

3.3. Interior packing density

Logically, a question arises: what is the packing density of RCPHS without boundary effects? Since boundary effects is totally eliminated, such a packing density should represent the space occupation efficiency of spheres in interior of the random close packing assembly of hard spheres and could be termed "interior packing density" of RCPHS. We try to deduce this interior packing density by assign the virtual hard container the ability to cut spheres on its wall (Fig. 4b),

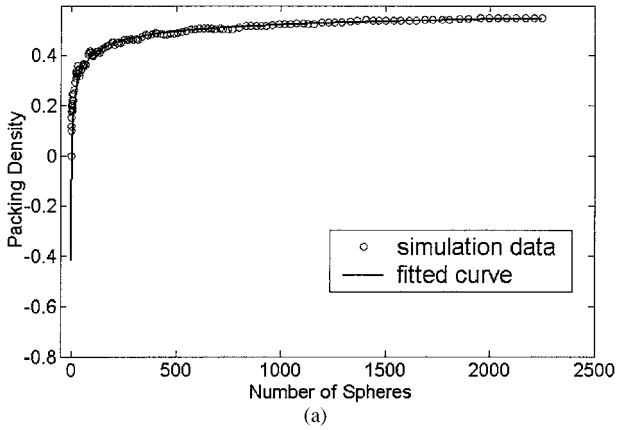

(a)

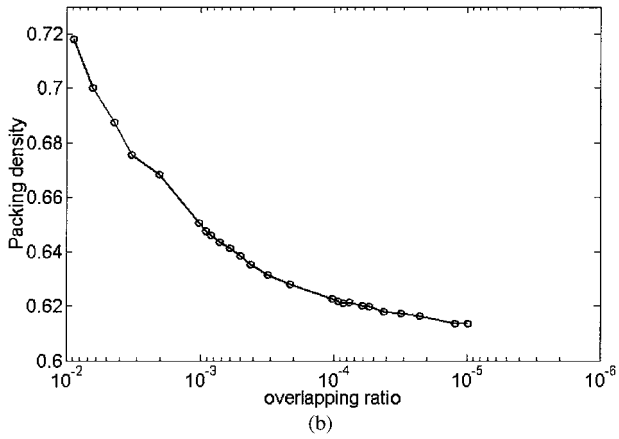

(b)

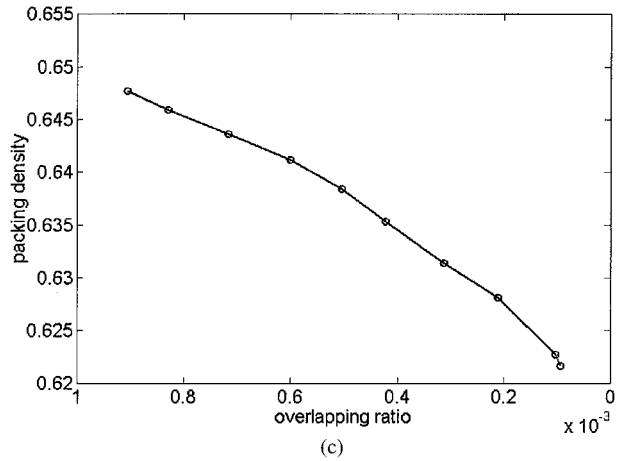

(c)

Figure 5 (a) Packing density ρ_1 as a function of N, number of spheres within virtual containers, $s = 5.0 * 10^{-4}$, (b) Evolution of $\rho_{1\infty}$ with overlapping ratio in semi-log plot; (c) Evolution of $\rho_{1\infty}$ with overlapping ratio in linear plot.

so that portion of these spheres within the container contributes to the sum of sphere's volume within the container. We define packing density $\rho_2(N)$ as the ratio of this volume to the volume of container. The key feature of the definition of $\rho_2(N)$ is that spheres with their center locate within a spherical shell of thickness $2r$ contribute part of their volume to the sum of sphere's volume within the container but only those within the inwards spherical shell of thickness r contribute to the N-counting (Fig. 6). Relationship between ρ_2 and N, number of spheres with their centers within containers is showed in Fig. 7. It is evident that ρ_2 reaches a stable value very quickly, in sharp contrast to ρ_1 which has a

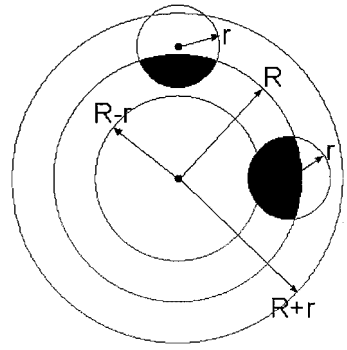

Figure 6 Schematic illustration of definition of $\rho_2(N)$. The radius of spheric container is R, and radius of packing sphere is r. If a sphere's center locates within the inward spheric shell of thickness r, it contributes to N-counting and sum of sphere volume. If a sphere's center locates within the outwards spheric shell of thickness r, it does not contribute to N-counting but to sum of sphere volume.

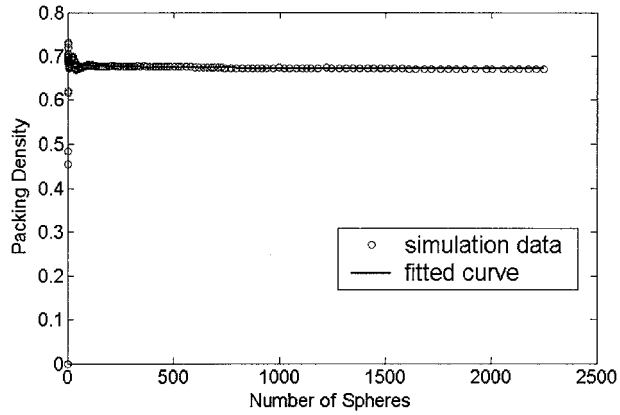

Figure 7 Packing density ρ_2 as a function of N, number of spheres with their centers within virtual container.

clear asymptotic characteristics. We try to fit $\rho_2(N)$ via N curve with a formula

$$\rho_2(N) = \rho_{2\infty} + BN^{-\frac{1}{3}} \tag{2}$$

where $\rho_{2\infty}$ is the extrapolation value of $\rho_2(N)$ as $N \to \infty$ (infinite number of spheres). By standard curve fitting technique, five sets of RCPHS of equal spheres in this work give an average $\rho_{2\infty}$ value of 0.6670 with a standard deviation of 0.0031 and an average B value of 0.033 with a standard deviation of 0.035.

By our definition, average volume contribution of each N-counting of partial sphere is

$$\bar{v} = \frac{\int_{R-r}^{R+r} v(x) 4\pi x^2 k \, \mathrm{d}x}{\int_{R-r}^{R} 4\pi x^2 k \, \mathrm{d}x} \tag{3}$$

where k is the average number of sphere centers in unit volume, x is the distance between centers of container and sphere, $v(x)$ is the volume of partial spheres within the container and R is the radius of container. Calculation shows that $\bar{v}$ equals $\frac{4}{3}\pi r^3$ (volume of a full sphere) and is independent of R. In other words, each N-counting, no matter whether the corresponding sphere center is in the inwards spherical shell or not, introduce statistically volume of a full sphere to the sum of sphere volume. This is the reason that $\rho_2(N)$ stabilizes

rapidly after first fluctuation with small N. Hypothesis test (more precisely, t-test) shows that the difference of average B value from zero is not significant at significant level of 0.05. All these analysis indicate that $\rho_{2\infty}$ is a density without boundary effects and can be considered as interior packing density of RCPHS.

3.4. Packing densities deduced from Voronoi diagram

Given a set of distinct points in three dimensional space, their Voronoi diagram divides the space according to the nearest-neighbor rule: Each point is associated with the region of space closest to it [18]. These regions are convex polyhedrons and are called Voronoi cells. This set of Voronoi cells is space-filling and non-overlapping. If the point set to generate Voronoi diagram is consisted of the centers of hard spheres in a random close packing, we get a Voronoi diagram based on RCPHS (VD-RCPHS), which is a useful tool to analysis connectivity of spheres in RCPHS [11, 12]. In VD-RCPHS, each sphere is enclosed in its Voronoi cell.

Since a Voronoi cell contains all points nearer to its sphere center than to others, its volume is a measure of the corresponding sphere's ability to occupy space in RCPHS structure. The ratio of volume of ith sphere to volume of its Voronoi cell, $\rho_v(i)$, presents the spatial occupancy efficiency of the ith sphere. So the packing density of RCPHS can be traced to individual sphere, or equivalently, to individual Voronoi cell. We consider $\rho_v(i)$ as the local packing density of RCPHS for ith sphere within ith Voronoi cell. Histogram of ρ_v is shown in Fig. 8. ρ_v ranges from about 0.5261 to about 0.7723 and peaks at about .06731.

It is well known that ordered close packing of equal spheres leads to a bulk packing density of 0.7405, the upper limit of density that cannot be exceeded. In such a ordered structure, local density is the same as bulk density. However, local density may be higher than 0.7405 in structures without translational symmetry, although their bulk densities will inevitably lower than that of ordered close packing. Indeed, the densest packing of twelve spheres around one is a regular icosahedron (with the twelve spheres at the vertices), a configuration cannot be incorporated into translational symmetric structure [11]. We checked spheres with local densities higher than 0.74 and found that they all overlap with their neighbors. Difference between diameter of a sphere and distance to its neighbor, a measure of linear overlapping, is in the order of $2 * 10^{-2}$. This again shows clearly the shortcoming of our algorithm and, perhaps, that of similar relocation algorithms adopted in literature [14]. Local density ρ_v is a sensitive quantity to detect and evaluate the influence of minute overlapping. We also calculate the quantity

$$\rho_z = \frac{\text{sum of volume of spheres}}{\text{sum of volume of Voronoi cells}} \qquad (4)$$

From five sets of RCPHS, we have an average value of $\rho_z = 0.6690$ with a standard deviation of 0.0006. It is evident that $\rho_{2\infty}$ and ρ_z is almost the same. Since each set of RCPHS is subjected to both $\rho_{2\infty}$ and ρ_z calculation, our analysis procedure is a typical randomized complete block experimental design [19]. Corresponding F-test [19] proves that difference between $\rho_{2\infty}$ and ρ_z is not significant at the significant level of 0.05.

The meaning of ρ_z is illustrated in Fig. 4c. Spheres are packed in a virtual container with rough wall that is built of faces of Voronoi polyhedrons. Since Voronoi cell is an exact description of spatial occupancy by spheres, ρ_z is a packing density without the effect of additional void near container walls, while such void exists near regular (plane or spherical) walls in traditionally defined bulk density. This is the reason that ρ_z and $\rho_{2\infty}$ have same value. In other words, There does exist a quantity as interior packing density of RCPHS which is a property of RCPHS without boundary effects and can be defined by either $\rho_{2\infty}$ or ρ_z.

Further more, because of the difficulty to interpret bulk density of RCPHS without ambiguity due to boundary effects, interior packing density may be a more appropriate indicator of the nature of random packing of hard spheres. It is noted that standard deviation of ρ_z is considerably less than that of $\rho_{1\infty}$. This suggests that ρ_z may be calculated more accurately and may be more sensitive to the random packing characteristics. We leave the study of random packing of spheres of equal size or unequal size with different packing densities to future work.

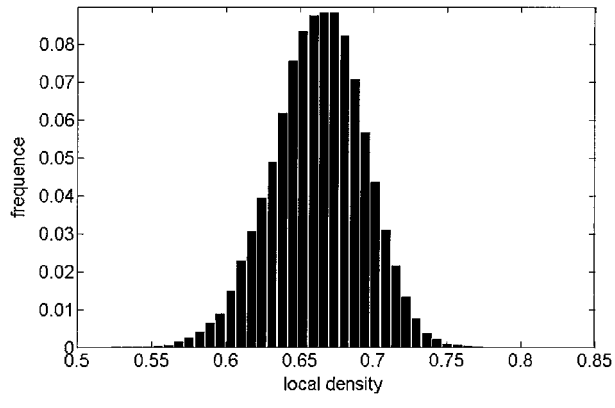

Figure 8 Histogram of local density for spheres in RCPHS structure.

4. Conclusion

In conclusion, we have presented a study on packing density of random close packing of equal hard spheres. The RCPHS is generated by a rearrangement algorithm with an optimization subroutine. Various packing densities are calculated on packing with overlapping ratio of $5 * 10^{-4}$. Traditionally defined packing density, bulk density, is found to be 0.635 ± 0.002 in this study. We propose the concept of interior packing density of RCPHS, which is the packing density without boundary effect. Interior packing density is calculated by two methods, resulting in values without statistically significant difference. Interior packing density deduced from Voronoi diagram is 0.6690 ± 0.0006. Using Voronoi diagram based on RCPHS, local packing density can be assigned to individual sphere and it ranges from

0.5261 to 0.7723, which is sensitive to sphere's local configuration and overlapping.

References

1. J. D. BERNAL, *Proc. Roy. Soc.* A **280** (1964) 299.
2. J. D. BERNAL and J. L. FINNEY, *Disc. Jaraday Soc.* **43** (1967) 62.
3. K. ITO, H. NAKAMURA, H. YOSIDA and N. ISE, *J. Amer. Chem. Soc.* **110** (1988) 6955
4. G. D. SCOTT, *Nature* **188** (1960) 908.
5. J. D. BERNAL and J. MASON, *ibid.* **188** (1960) 910.
6. R. RUTGERS, *ibid.* **193** (1962) 465.
7. G. D. SCOTT and D. M. KILGOUR, *J. Phys.* D **2** (1969) 863.
8. G. Q. LU and X. SHI, *J. Mater. Sci. Lett.* **13** (1994) 1709.
9. C. H. BENNETT, *J. Appl. Phys.* **43** (1972) 2727.
10. W. S. JODREY and E. M. TORY, *Phys. Rev.* A **32** (1985) 2347.
11. A. S. CLARKE and J. D. WILEY, *ibid.* B **35** (1987) 7350.
12. S. D. CLARKE and H. JONSSON, *ibid.* E **47** (1993) 3975.
13. J. L. FINNEY, *Mater. Sci. & Eng.* **23** (1976) 199.
14. D. HE and N. N. EKERE, *J. Mater. Sci. Lett.* **17** (1998) 1723.
15. G. LIU and K. E. THOMPON, *Powder Technology* **113** (2000) 185.
16. ZHIGANG FAN, "Computer Simulation of Polycrystalline Material Structure" (Thesis for Bachelor's Degree, Tianjin University, Tianjin, China, June 2001).
17. Y. YUAN, "Numerical Method For Nonlinear Programming" (Shanghai Scientific & Technical Publishers, Shanghai, 1993, in Chinese) p. 207.
18. FRANZ. AURENHAMMER, *ACM Computing Surveys* **23** (1991) 345.
19. DOUGLEAS C. MONTGOMERY, "Design and Analysis of Experiments" (John Wiley & Sons Inc., USA, 1984) p. 123.

Received 17 December 2001
and accepted 4 March 2003